

Accepted Manuscript

Title: Effects of cultured *Cordyceps* mycelia polysaccharide A on tumor neurosis factor- α induced hepatocyte injury with mitochondrial abnormality

Author: <ce:author id="aut0005"
author-id="S0144861717300206-
eeb39cb1f4cd3d09702b829db6803fff"> Huiling
Tang<ce:author id="aut0010"
author-id="S0144861717300206-
98ad71373043388404c3e4b2fee2e3a1"> Weikun
Wei<ce:author id="aut0015"
author-id="S0144861717300206-
275e81903cdef7d0c5f052c118a35854"> Wang
Wang<ce:author id="aut0020"
author-id="S0144861717300206-
16202160cfc5db66b0926ee7fabde3b8"> Zhengqi
Zha<ce:author id="aut0025"
author-id="S0144861717300206-
8d1bc6b9a466b3bc360e3c2b61d98a5a"> Ting Li<ce:author
id="aut0030" author-id="S0144861717300206-
3ee95b825e61eb3f56052a3b80c77e18"> Zhijie
Zhang<ce:author id="aut0035"
author-id="S0144861717300206-
1fb67eb8c86d448cb2d0669f8bea80ab"> Chen Luo<ce:author
id="aut0040" author-id="S0144861717300206-
d8dd16710e218f5657bf50d2706a3347"> Hongping
Yin<ce:author id="aut0045"
author-id="S0144861717300206-
07b54cde2e0050ac67d7e1f880fcf2e3"> Fengjie
Huang<ce:author id="aut0050"
author-id="S0144861717300206-
b440db44b623e039eef05f316b82156d"> Ying
Wang

PII: S0144-8617(17)30020-6
DOI: <http://dx.doi.org/doi:10.1016/j.carbpol.2017.01.019>
Reference: CARP 11897

To appear in:

Received date: 21-7-2016

Revised date: 4-1-2017

Accepted date: 4-1-2017

Please cite this article as: Tang, Huiling., Wei, Weikun., Wang, Wang., Zha, Zhengqi., Li, Ting., Zhang, Zhijie., Luo, Chen., Yin, Hongping., Huang, Fengjie., & Wang, Ying., Effects of cultured Cordyceps mycelia polysaccharide A on tumor neurosis factor- α induced hepatocyte injury with mitochondrial abnormality. *Carbohydrate Polymers* <http://dx.doi.org/10.1016/j.carbpol.2017.01.019>

This is a PDF file of an unedited manuscript that has been accepted for publication. As a service to our customers we are providing this early version of the manuscript. The manuscript will undergo copyediting, typesetting, and review of the resulting proof before it is published in its final form. Please note that during the production process errors may be discovered which could affect the content, and all legal disclaimers that apply to the journal pertain.

Effects of cultured *Cordyceps mycelia* polysaccharide A on tumor neurosis factor- α induced hepatocyte injury with mitochondrial abnormality

Huiling Tang^{1,2,#}, Weikun Wei^{1,#}, Wang Wang³, Zhengqi Zha¹, Ting Li⁴, Zhijie Zhang¹, Chen Luo¹, Hongping Yin¹, Fengjie Huang^{1,*}, Ying Wang^{1,*}

¹ School of Life Science and Technology, State Key Laboratory of Natural Medicines, China Pharmaceutical University, Nanjing 210009, People's Republic of China

² Department of Pharmacy, Jiangsu Food & Pharmaceutical Science College, Huaian 223003, People's Republic of China

³ Basic Medical College, Nanjing University of Chinese Medicine, Nanjing 210046, People's Republic of China

⁴ School of Pharmaceutical Sciences, Shandong University, Jinan 250012, People's Republic of China.

#Both the authors worked equally to this work.

*Corresponding authors: hfj@cpu.edu.cn (FJ Huang); ywang@cpu.edu.cn (Y Wang)

Postal address: No. 24 Tongjiaxiang Road, Nanjing 210009, Jiangsu, People's Republic of China

Tel: +86 025 83271108;

Fax: +86 025 83271249.

Highlights

- CPS-A was isolated by 65% alcohol extraction and ion-exchange chromatography.
- CPS-A was composed of $\rightarrow 2$)- β -D-manp-(1 \rightarrow , $\rightarrow 2$, 4)- β -D-manp-(1 \rightarrow , and (1 \rightarrow 4)-linked α -D-Glcp.
- CPS-A protected TNF- α induced mitochondria abnormality via TNFR1/ROS/Mfn2 pathway.
- CPS-A could up-regulate Mfn2, PGC-1 α , and membrane potential.
- CPS-A released TNF- α induced apoptosis and ROS production in L02 cells.

Abstract

Cordyceps sinensis mycelia polysaccharide A (CPS-A), was isolated from cultured *Cordyceps* mycelia by 65% alcohol extraction and ion-exchange column chromatography. The molecular weight of CPS-A was 1.2×10^4 Da and the backbone was mainly composed of (1 \rightarrow 2)-linked β -D-mannopyranose, (1 \rightarrow 2,4)-linked β -D-mannopyranose and (1 \rightarrow 4)-linked α -D-glucopyranose with terminal β -D-mannopyranose and α -D-glucopyranose residues. CPS-A played a protective role against TNF- α induced mitochondria injury in L02 cells via up-regulation of mitofusin 2, peroxisome proliferator-activated receptor gamma coactivator 1-alpha (PGC-1 α), and membrane potential. CPS-A also played a protective role against TNF- α induced L02 cells apoptosis via up-regulation of Bcl-2 and down-regulation of Bid, Bax, cleaved caspase-3, cleaved caspase-9 and ROS production. Moreover,

CPS-A attenuated both the normal expression and overexpression of TNF- α receptor 1 (TNFR1) induced by TNF- α administration. In conclusion, CPS-A was involved in TNF- α induced mitochondria abnormality via TNFR1/ROS/Mfn2 pathway.

Key words: *Cordyceps sinensis* mycelia polysaccharide A; Mitochondria abnormality; TNF- α receptor 1; Mitofusin 2; Apoptosis

1. Introduction

Mitochondrial abnormality is associated with the development of nonalcoholic fatty liver, which causes life-threatening liver damage (Hikita et al., 2015; Kathirvel, Morgan, French, & Morgan, 2013). Mitochondria play an important role in free radical production, energy metabolism, aging and cell apoptosis. Mitofusin-2 (Mfn2) is a mitochondrial membrane protein that participates in mitochondrial fusion and contributes to the maintenance and operation of the mitochondrial network (Bach et al., 2003). Mitochondria fusion could preserve cells from death while apoptosis restrains mitochondria fusion. Therefore, inhibition of hepatocyte apoptosis and amelioration of liver damage might be regulated by Mfn2 (De Brito & Scorrano, 2008). Peroxisome proliferator-activated receptor gamma co-activator (PGC)-1 α is a thermogenic transcriptional co-activator, which is involved in energy metabolism through regulation of mitochondrial biogenesis and respiration (Wu et al., 1999). Li et al. (2004) found that the overexpression of Mfn2 decreased hepatic injury in livers and L02 cells treated with TNF- α , however, without up-regulating PGC-1 α .

TNF- α is a cell signaling protein involved in systemic inflammation, which is ascribed to induce ROS production in mitochondria, as well as to alter mitochondrial function by impairing membrane permeability (Busquets et al., 2003). TNF- α interacts with two cognate receptors: TNF receptor type 1 (TNFR1) and TNF receptor type 2 (TNFR2). TNFR1 is ubiquitously expressed in most tissues, and it can be fully activated by both the membrane-bound and soluble trimeric forms of TNF; in addition, TNFR2 is found only in cells of the immune system, responding to the membrane-bound form of the TNF homotrimer (Desmouliere & Guyot, 2004).

Cordyceps sinensis, a traditional Chinese medicine, has been used for thousands of years to maintain health and treat a wide range of disorders (Yan, Wang, & Wu, 2014). Polysaccharides extracted from *C. sinensis* had significant activities in the treatment of tumor, oxidative effects, renal dysfunction, and liver disease (Shashidhar, Giridhar, Sankar, & Manohar, 2013). Peng et al. (2013) found that a polysaccharide extracted from *C. sinensis* had a potent effect on anti-liver fibrosis associated with the inhibition of HSC activation and TGF- β 1/Smads signaling pathway. Our group reported that *C. sinensis* polysaccharide CPS-2 and its active fragment CPS-F showed protective effects against renal injury and kidney inflammation. Since the underlying molecular mechanism of hepatocyte injury caused by mitochondria-associated apoptosis remains unclear in our previous studies (Wang et al., 2014b; Wang et al., 2015), an active polysaccharide CPS-A was extracted by 65% ethanol at pH 2.0 in the present study, and the mechanism of its remarkable protective effects were also studied.

Mitochondrial impairment is hypothesized to contribute to the pathogenesis of chronic liver diseases. Li et al. (2014) reported that TNF- α induced down-regulation of Mfn2 and PGC-1 α in a rat liver IRI model, which was associated with hepatic mitochondrial swelling, increased levels of ROS and alanine aminotransferase (ALT) activity, as well as L02 cell apoptosis. Wang et al. (2012) reported that the protective effect of water extracts of *Cordyceps sinensis* against *t*-BHP-induced HepG2 cells might be a result of the reduction of ROS, the modulation of Bcl-2 and Bax, mitochondrial membrane potential and SOD activity in hepatocytes. Additionally, the overexpression of Mfn2 effectively attenuated mitochondrial fragmentation and reversed the mitochondrial damage observed in glycochenodeoxycholic acid treated L02 cells (Chen et al., 2013). Taken together, these findings indicate that the pathogenesis of the liver damage is highly associated with mitochondrial abnormality, the loss of Mfn2, and ROS accumulation. In order to clarify the mechanism of the action of CPS-A in suppressing liver damage, we hypothesized that CPS-A relieved TNF- α -induced hepatocyte apoptosis through the TNFR1/ROS/Mfn2 signaling pathway in the present study. We have investigated the effects of CPS-A against TNF- α -induced mitochondrial abnormality on L02 cells and explored its effects of CPS-A on mitochondria-associated targets, apoptosis-related proteins, and the TNF- α receptors.

2. Materials and methods

2.1. Materials

Cultured *Cordyceps sinensis* mycelia were obtained from Changxing

Pharmaceutical Co. Ltd., Zhejiang, China. The material was identified as *Cephalosporium sinense* Chen, one kind of *C. sinensis*, by the Institute of Microbiology, Chinese Academy of Sciences (Microbiological Detection Report no.169, 2004). Mannose, rhamnose, glucose, galactose, arabinose, xylose, glucuronic acid, galacturonic acid, ribose, fucose and 1-phenyl-3-methyl-5-pyrazolone (PMP) were purchased from Sigma-Aldrich (St. Louis, USA). Dextran standards (*M_w* 805,000, 393,000, 210,000, 48,800, 21,700, 10,000, 6,000, and 180) were purchased from Shodex Co. Ltd (Shodex, china). All other reagents were of analytical grade. Cell culture materials were obtained from Gibco-BRL (Rockville, MD, USA). Human recombination TNF- α was purchased from PeproTech (Rocky Hill, NJ, USA). Reagents used for reverse transcription PCR were purchased from Bio-Rad Corporation (Hercules, California, USA). TRNzol Plus was from Biouniquer Corporation (Jiangsu, China). Rhodamine-123 was purchased from Beyotime (Nanjing, China).

2.2. Isolation and purification of CPS-A

C. sinensis was refluxed for 2 h in eight-fold 95% ethanol (m/v) to remove fats. The residue was refluxed again for 3 h in ten-fold 65% ethanol (m/v) at pH 2.0. Then the supernatant was adjusted to pH 7.0 and precipitated with 95% ethanol until the final concentration of ethanol was up to 75%. Crude polysaccharide was deproteinized with Sevag reagent (Savag, Lackman, & Smolens, 1938). After dialysis and lyophilization, the crude polysaccharide was dissolved and loaded onto a DEAE-cellulose 52 column (4.5×30 cm). One main fraction eluted by distilled water

was collected and further purified on a Sephadex G-50 column (1.0×80 cm) eluted with distilled water to get one polysaccharide fraction, which was designated as CPS-A.

2.3. Purity and molecular weight of CPS-A

Purity and molecular weight were estimated by high performance gel permeation chromatography (HPGPC) in 0.1 M NaNO₃ at 30°C. Shodex columns (OHpak SB-805, SB-802) were used and the flow rate was 0.35 mL/min. CPS-A was dissolved in 0.1 M NaNO₃, and the solution (2 mg/mL, 80 µl) was injected. Dextran standards were used to establish a standard curve with GPC software.

2.4. Monosaccharide constituents of CPS-A

High performance liquid chromatography (HPLC) was conducted to identify the monosaccharides by the PMP-labeling procedure as described previously (Dai et al., 2010). Briefly, 5 mg CPS-A was hydrolyzed by 2 M TFA for 2 h at 100°C. After removing TFA, the hydrolysate was derivatized through the addition of 0.6 M NaOH (25 µl) and 0.4 M PMP (50 µl). Afterward, the solution was neutralized with 50 µl of 0.3 M HCl and extracted with chloroform three times. The aqueous phase was loaded into a ZORBAX Eclipse XDB-C18 (250 mm×4.6 mm) column with an acetonitrile to phosphate buffer (pH 6.7) ratio of 17:83 (v/v). Flow rate was 1 mL/min. The ten standard monosaccharides were labeled by the same procedure.

2.5. FT-IR analysis

The mixture of 2 mg CPS-A and 200 mg KBr powder was ground slightly under infrared lamp, and then was flaked to be scanned by Nicolet Impact 410 FT-IR from

4000 cm^{-1} to 400 cm^{-1} .

2.6. Methylation and GC-MS analysis

The CPS-A was methylated according to the Ciucanu method (Ciucanu & Kerek, 1984). The methylated residues were hydrolyzed with 2 M TFA. The hydrolysates were reduced with NaBH_4 . The partially methylated alditol acetates were analyzed by GC-MS (HP 6890 II, Agilent USA). The acetylated derivatives were loaded into a DB-225MS capillary column. The temperature of Ramp 1 was elevated from 160°C to 210°C at a rate of 2°C/min, then remained unchanged for 8 min, and the temperature of Ramp 2 was ramped from 210°C to 240°C at a rate of 5°C/min, then kept at 240°C for 6 min.

2.7. NMR spectroscopy

CPS-A (40 mg) was dissolved in 99.99% D_2O . 1D (^1H and ^{13}C) NMR and 2D NMR, including ^1H - ^1H Correlated Spectroscopy (^1H - ^1H COSY), Heteronuclear Singular Quantum Correlation (HSQC), and Heteronuclear Multiple Bond Correlation (HMBC) spectra were measured at 25°C with JEOL JNM-ECP 600 NMR spectrometer (JEOL, Tokyo, Japan). All chemical shifts were in reference to acetone- d_6 .

2.8. Biological activity

2.8.1. Cell culture

Human hepatocyte HL-7702 (L02) was purchased from cell resource center of Institutes of Biomedical Sciences of Fudan University. L02 cells were cultured in Dulbecco's modified Eagle's medium (DMEM) supplemented with 10% fetal bovine

serum and 1% penicillin/streptomycin at 37°C in an incubator filled with 5% CO₂. L02 cells were pre-incubated with 10 mM glutathione (GSH, positive control) or CPS-A for 12 h, and then induced with 100 ng/mL TNF- α for additional 24 h.

2.8.2. Cell Viability Assay

MTT assay was carried out to determine the proliferation and growth viability of L02 cells (Hansen, Nielsen, & Berg, 1989). L02 cells were added in the 96-well plate at 5×10^5 cells/mL overnight. Different concentrations of TNF- α (0, 0.01, 0.1, 1, 10, 30, and 100 ng/mL), glutathione (GSH) (0, 0.1, 1, 5, 10, and 25 mM), or CPS-A (0, 12.5, 25, 50, 100, and 200 μ g/mL) were incubated for 24 h or 48 h at 37°C in the atmosphere with 5% CO₂. Each concentration was repeated in three wells. 20 μ l of 5 mg/mL MTT was added into each well and incubated for 4 h. Subsequently, 150 μ l of dimethyl sulfoxide was added into each well and the optical density (OD) was read at 570 nm by Microplate Reader (BioTek, USA).

2.8.3. Apoptosis measurement using DAPI staining

The cells in logarithmic growth phase were seeded in the 6-well plate, and treated with 100 ng/mL TNF- α for 24 h after pretreatment with 10 mM of GSH, 25, 50, and 100 μ g/mL of CPS-A for 12 h. 4% paraformaldehyde was added into each well, and fixed at room temperature. Finally, the cells were stained by DAPI under dark condition for 15 min after rinsing with PBS three times, and then were observed under an IX51 inverted fluorescence microscope (Olympus, Japan).

2.8.4. ROS expression level using DCFH-DA fluorescence probe

L02 cells were added to the 6-well plate, and incubated with 10 mM of GSH, 25,

50, or 100 µg/mL of CPS-A for 12 h, then were treated with 100 ng/mL TNF-α for 24 h. DCFH-DA (2', 7'-dichlorofluorescein-diacetate) was added into each well, and reacted at 37°C for 20 min. Then L02 cells were shed using pancreatin without EDTA, rinsed with PBS three times and resuspended. Subsequently, flow cytometry was performed to detect ROS generation at an excitation wavelength of 488 nm and an emission wavelength of 525 nm.

2.8.5. Mitochondrial membrane potential assay

Mitochondrial membrane potential was measured by Rhodamine-123, an indicator of mitochondrial membrane potential (Lemasters & Nieminen, 1997). Briefly, L02 cells in the logarithmic growth phase were added in the 6-well plate at 1×10^5 cells/mL and stimulated by 100 ng/mL TNF-α for 24 h after pretreatment with 10 mM of GSH, 25, 50, or 100 µg/mL of CPS-A for 12 h. Rhodamine-123 was added to the cells until the concentration reached 10 µg/mL to cultivate at 37°C in the atmosphere of 5% CO₂ for 20 min. The cells were resuspended in the medium or PBS several times and the fluorescence intensity was assessed by an Accuri C6 cell flow cytometry (BD Biosciences, Franklin Lakes, NJ, USA).

2.8.6. Real-Time PCR

Total RNA was detached from L02 cells and RNA concentration was quantified by Microplate Reader at 260 nm after being dissolved in DEPC water. cDNA was acquired through the transcription of mRNA using olig(dT) 18 primer via BU-SuperScript RT KIT (Biouniquer) according to the manufacturer's instructions. Real-Time PCR was operated using an ABI 7700 Prism Sequence Detection System

and TaqMan primer probes (Applied Biosystems, Foster City, CA, USA). GAPDH was used as the loading control. Sequences of the primers were as follows: Mfn2 forward primer, 5'-GACCCCGTTACCACAGAAGA-3' and reverse primer, 5'-GCAGAACTTTGTCCCAGAGC-3'; PGC-1 α forward primer, 5'-CCTGCATGAGTGTGTGCTCT-3' and reverse primer, 5'-GCAAAGAGGCTGGTCTTCAC-3'; TNFR1 forward primer, 5'-TGCCAGGAGAAACAGAACA-3' and reverse primer, 5'-AACCAATGAAGAGGAGGGAT-3'; TNFR2 forward primer, 5'-CTCACTTGCCTGCCGATAA-3' and reverse primer, 5'-CCCTTCTGTCCAACGCACT3'; and GAPDH forward primer, 5'-ATGGTGGTGAAGACGCCAGT-3' and reverse primer, 5'-GCACCGTCAAGGCTGAGAAC-3'.

2.8.7. Western blot

L02 cells were harvested and lysed in RIPA buffer. Ninety micrograms of proteins were loaded into each lane of a 10% sodium dodecyl sulfate (SDS)-polyacrylamide gel and transferred onto polyvinylidene fluoride (PVDF) membranes (Bio-Rad, Hercules, CA, USA). The following antibodies were used: β -actin (Epitomics, USA); TNFR I, Mfn2, and Bid (Abcam, UK); cleaved caspase-3, cleaved caspase-9, Bax, and Bcl-2 (Cell Signaling, USA). Protein expression levels were detected using an enhanced chemiluminescence (ECL) system (BeyoECL Plus, Beyotime). Immunoblotted bands were quantified using Gel-Pro Analyzer 4.0 software (Media Cybernetics, Rockville, MD, USA) and the protein of interest was

normalized to β -actin.

2.8.8. *pGL3-TNFR1 promoter construction*

On the basis of the GenBank sequence of Homo sapiens TNFR1 NC_000012.12, the TNFR1 promoter was amplified by PCR using the specific forward primer (TCTCTCGAGAGAGTGAGGCAGTGTTGCA) and reverse primer (TCTACGCGTCTTTGTGATGGTGGTGAGC). Both purified PCR products and pGL3-Basic vector were conducted to react with XhoI and MluI at 37°C for 3 h and connected with T4 Ligase at a ratio of 1:3 at 16°C overnight. The pGL3-TNFR1 promoter was transformed into *E.coli* DH5 α competent cells and then cultivated with 50 μ g/mL Amp at 37°C for 12~48 h. The pGL3-TNFR1 promoter vectors were transfected with LipofectamineTM 2000 to L02 cells in 24-well plates with DMEM free antibiotics for 10 h. Meanwhile, pGL3-Basic was transfected as a negative control and pGL3-SV40 as a positive control. The L02 cells were pre-treated with various concentrations of CPS-A (25, 50, 100 μ g/mL) for 12 h prior to 100 ng/mL TNF- α stimulation for an additional 24 h. Fluorescence intensity of luciferase reporter vectors were determined by Microplate Reader (BioTek Instruments, USA).

2.9. *Statistical analysis*

Data were expressed as mean \pm standard error of the mean (SEM). Differences were analyzed using one-way analysis of variance (ANOVA), followed by Student–Newman–Keuls post hoc multiple comparison tests. A *p* value less than 0.05 was considered statistically.

3. Results

3.1. Isolation, purification, and monosaccharide composition of CPS-A

CPS-A was obtained by 65% ethanol solution extraction at pH 2.0. Showed as light yellow powder, CPS-A's yield was 11.0%. HPGPC was used to determine the homogeneity and molecular weight of the polysaccharide. A single symmetrical peak was shown (Fig. 1A), suggesting that CPS-A was a homogeneous polysaccharide. It had no absorption peaks appeared at 280 or 260 nm, indicating that the absence of protein or nucleic acid. The molecular weight of CPS-A was 1.2×10^4 Da, as determined by the correlation with a dextran standard curve (Fig. 1B and 1C). A monosaccharide analysis conducted by the PMP precolumn derivation method showed that CPS-A was composed of mannose and glucose with the ratio of 11:2. (Supplementary data 1).

3.2. FT-IR spectroscopy analysis of CPS-A

The FT-IR spectrum of CPS-A was examined. The broad and intense bands at $3600-3200 \text{ cm}^{-1}$ were attributed to the symmetrical stretching vibration of O-H, identified as inter-molecular hydrogen bond due to the absence of the bands of intra-molecular hydrogen bond near 3560 cm^{-1} but the presence of the bands of inter-molecular below 3400 cm^{-1} (Hu, Liang, & Wu, 2015). The band at 1122 cm^{-1} was attributed to vibrations of C-O-C linkages. The band at 1055 cm^{-1} was the result of vibrations of C-O-H. The bands at 1638 cm^{-1} was attributed to the characteristic peak of bound water (Liu et al., 2016). The bands at $844 \pm 8 \text{ cm}^{-1}$ and $891 \pm 7 \text{ cm}^{-1}$ indicated the presence of α and β epimerides, respectively (Cai, Xie, Chen, & Zhang, 2013).

3.3. Methylation and GC-MS analyses of CPS-A

CPS-A was methylated and converted into five main types of alditol acetates at a relative ratio of 4.4:17.1:43.7:27.5:7.4 (Table 1). GC-MS chromatograms of methylated sugars of CPS-A were shown in Supplementary data 2. 2,4,5-tetra-*O*-acetyl-3,6-di-*O*-methyl-mannitol was originated from \rightarrow 2, 4)-Manp-(1 \rightarrow , indicating that CPS-A contains a branched structure. 1,5-di-*O*-acetyl-2,3,4,6-tetra-*O*-methyl-Manp and 1,5-di-*O*-acetyl-2,3,4,6-tetra-*O*-methyl-Glcp were originated from Manp-(1 \rightarrow and Glcp-(1 \rightarrow , respectively. Terminal Manp and terminal Glcp existed in the end of main chain or branched chain. Combining weight-average molecular weight and molar proportion, it can be speculated that the main chain of CPS-A was comprised of \rightarrow 2)-Manp-(1 \rightarrow , \rightarrow 2, 4)-Manp-(1 \rightarrow , and \rightarrow 4)-Glcp-(1 \rightarrow residues.

3.4. NMR spectroscopy analysis of CPS-A

^1H NMR spectrum was used to preliminarily identify the categories of glycosidic bonds of polysaccharides (Makarova et al., 2013). There existed both α -configuration and β -configuration in CPS-A (Fig. 2A). The anomeric proton signals at δ 5.15 and 5.10 were attributed to α -configuration units in pyran ring, while the signals at δ 4.99, 4.85, and 4.90 were attributed to β -configuration (Dang et al., 2013). Other proton signals were situated in the range of δ 3.09-4.01, which were assigned to H2–H6 of the sugar residues.

According to different chemical shifts of carbon, we can determine not only the location of the various chemical environment of carbon, but also the molecular

configuration and conformation (Ruthes et al., 2013). The ^{13}C NMR spectrum of CPS-A (Fig. 2B) can be divided into three regions: δ 90~95 for the anomeric carbon C-1; δ 70~75 for C-2, C-3, C-4, and C-5; and δ 60~70 for C-6. The anomeric carbon signals appeared at δ 102.54, 102.20, 102.12, and 100.49, suggesting *O*-linking with C-1 (Li et al., 2013). The signal at δ 100.49 was attributed to $\rightarrow 4$)- α -D-Glcp-(1 \rightarrow); the signal at δ 102.12 was assigned to $\rightarrow 2$)- β -D-Manp-(1 \rightarrow ; and the signal at δ 100.54 was attributed to α -D-Glcp-(1 \rightarrow . Signals at δ 78.83, 78.77, 78.74, and 78.62 indicated *O*-linking with C-2, C-3, C-4, and C-5 substituted to varying degrees. The chemical shifts were shown in Table 2.

HSQC spectrum provides the connectivity information between carbons and its attached protons (Nie et al., 2011). Taken HSQC spectrum (Fig. 2D) together with ^1H - ^1H COSY spectrum (Fig.2C), signals of H-1/C-1 at δ 5.10/100.49, 4.85/102.12, 4.90/102.20, 5.15/100.54, and 4.99/102.20 were assigned to five main glycosyl types including $\rightarrow 4$)- α -D-Glcp-(1 \rightarrow , $\rightarrow 2$)- β -D-Manp-(1 \rightarrow , $\rightarrow 2,4$)- β -D-Manp-(1 \rightarrow , α -D-Glcp-(1 \rightarrow and β -D-Manp-(1 \rightarrow , respectively. Signals of H-6/C-6 at δ 3.61/60.99, 3.80/64.74, and 3.61/60.99 were assigned to $\rightarrow 2$)- β -D-Manp-(1 \rightarrow , α -D-Glcp-(1 \rightarrow , and $\rightarrow 2,4$)- β -D-Manp-(1 \rightarrow , respectively. Signals of H-5/C-5 at δ 3.80/69.92 and 3.90/78.74 were assigned to $\rightarrow 4$)- α -D-Glcp-(1 \rightarrow and β -D-Manp-(1 \rightarrow , respectively. Signals of H-3/C-3 at δ 3.69/73.15 and 3.66/78.43 were assigned to β -D-Manp-(1 \rightarrow and $\rightarrow 2,4$)- β -D-Manp-(1 \rightarrow , respectively.

HMBC spectrum gives correlations between carbons and protons that are separated by two or three bonds (Shang et al., 2012). Signals at δ 5.15/73.15 were

assigned to H-1 of β -D-Glcp-(1 \rightarrow) and C-2 of \rightarrow 2, 4)- β -D-Manp-(1 \rightarrow). Signals at δ 5.03/73.15 were assigned to H-2 of \rightarrow 2)- β -D-Manp-(1 \rightarrow) and C-2 of \rightarrow 2, 4)- β -D-Manp-(1 \rightarrow). Signals at δ 4.99/78.43 were assigned to H-1 of β -D-Manp-(1 \rightarrow) and C-3 of \rightarrow 2, 4)- β -D-Manp-(1 \rightarrow). Signals at δ 5.03/102.20 were assigned to H-2 of \rightarrow 2)- β -D-Manp-(1 \rightarrow) and C-1 of \rightarrow 2, 4)- β -D-Manp-(1 \rightarrow). Signals at δ 4.85/78.76 were assigned to H-1 of \rightarrow 2)- β -D-Manp-(1 \rightarrow) and C-4 of \rightarrow 4)- α -D-Glcp-(1 \rightarrow). Signals at δ 4.85/71.02 were assigned to H-1 of \rightarrow 2)- β -D-Manp-(1 \rightarrow) and C-2 of \rightarrow 4)- α -D-Glcp-(1 \rightarrow) (Fig. 2E).

In summary, the molecular structure of CPS-A was predicted as follows: the main chain was composed of \rightarrow 2)- β -D-Manp-(1 \rightarrow), \rightarrow 2, 4)- β -D-Manp-(1 \rightarrow), and \rightarrow 4)- α -D-Glcp-(1 \rightarrow) residues with β -D-Manp-(1 \rightarrow) and α -D-Glcp-(1 \rightarrow) as terminal residues. The entire molecule was a kind of repetitive structure composed of segments.

3.5. Effects of CPS-A on TNF- α -induced L02 cell viability

TNF- α , involved in the systemic inflammatory response, is an important cytokine in the induction of apoptosis (Santos et al., 2016). The results of the present study indicated that TNF- α played an effectively suppressive role on L02 cells when the concentration was 30 ng/mL. TNF- α significantly reduced the proliferation of L02 cells at 100 ng/mL, which was chosen as the stimulation concentration (Fig. 3A). Similarly, 10 mM of GSH was chosen as the positive group (Fig. 3B). CPS-A at less than 100 μ g/mL had no inhibitory impact on the growth of L02 cells after treatment for 48 h (Fig. 3C). As shown in Fig. 3D, L02 cells were pre-incubated with CPS-A (25,

50, and 100 $\mu\text{g}/\text{mL}$) for 12 h prior to $\text{TNF-}\alpha$ treatment. Therefore, CPS-A could significantly relieve $\text{TNF-}\alpha$ -induced L02 injury in a dose-dependent manner.

3.6. Effect of CPS- A on the $\text{TNF-}\alpha$ -induced apoptosis

DAPI assay was employed to monitor cell apoptosis, in which a strong fluorescence signal was emitted when DAPI combined with DNA in the nucleus (Sourav, Soumya, & Samiran, 2014). As shown in (Fig. 4G), normal nuclei of cells had an intact round morphology and a clear outline. Cell shrinkage, membrane blebbing, chromatin condensation, and apoptotic bodies (arrows) appeared in $\text{TNF-}\alpha$ group. Pretreatment with GSH or CPS-A caused a statistically significant reduction in apoptosis compared with the control group. With the concentrations of CPS-A increasing, the number of normal cells raised and apoptotic bodies decreased.

3.7. CPS-A inhibited abnormal expression of apoptosis-related protein

To investigate whether CPS-A exerted protective effects on the expression of apoptosis-related protein, L02 cells were pre-treated with CPS-A (25, 50, and 100 $\mu\text{g}/\text{mL}$) for 12 h, respectively, then incubated with 100 ng/mL of $\text{TNF-}\alpha$. Compared with the model group, the protein expression of Bid and Bax were decreased in all treatment groups (Fig. 4A, 4B, and 4C), whereas Bcl-2 expression was reversed to normal levels by CPS-A pre-treatment (Fig. 4A and 4D).

To further elucidate the mechanism responsible for the anti-apoptosis effect of CPS-A, the expression levels of caspases were detected by Western blot (Fig. 4C and D). The results illustrated that the protein levels of cleaved caspase-3 and cleaved

caspase-9 were significantly increased, compared with the control group after stimulation of TNF- α (100 ng/mL). Moreover, CPS-A (50 and 100 μ g/mL) pre-treatment could significantly decrease the mRNA expression of cleaved caspase-3 and cleaved caspase-9 in a dose-dependent manner (Fig. 4E and 4F).

3.8. Effects of CPS-A on intracellular ROS production

Since many DNA damage-causing agents turns on the apoptosis pathway through ROS generation (Chen et al., 2013), the possibility that ROS increasing might be a key step in the TNF- α -induced apoptosis was evaluated in the present study. The down-regulated ROS production was determined by flow cytometric analysis using DCFH-DA as a fluorescence probe. Compared with TNF- α treated group, L02 cells exposed to CPS-A (25, 50, and 100 μ g/mL) showed significant decreases in the intracellular ROS in a dose-dependent manner (Fig. 5A and 5B).

3.9. CPS-A raised expression levels of Mfn2 and PGC-1 α in TNF- α -induced L02 cells

Mfn2, a sort of highly conserved transmembrane protein, mediates the fusion of mitochondria, and participates in various cell biological processes such as cell energy metabolism, cell apoptosis, and cell proliferation (Antonio, Isabel, David, & Pablo, 2015). In comparison with the model group, a significant rebound of mRNA expression occurred at 25 μ g/mL of CPS-A group. In addition, 50 and 100 μ g/mL of CPS-A exerted an influence on extremely rising expression level of Mfn2 by TNF- α -induced mitochondrion damage in L02 cells (Fig. 5E). Pre-treatment with CPS-A dramatically elevated Mfn2 expression in a dose-independent manner (Fig. 5C

and 5D), which was consistent with the results of Real-Time PCR experiment.

We further explored the influence of PGC-1 α on TNF- α -treated L02 cells. After TNF- α decreased the mRNA expression of PGC-1 α , CPS-A up-regulated the expression of PGC-1 α in a dose-dependent manner (Fig. 5F). In conclusion, CPS-A could significantly reverse the inhibited expression of Mfn2 and PGC-1 α caused by TNF- α .

3.10. Analysis of mitochondrial membrane potential in TNF- α -treated L02 cells

The mitochondrial membrane potential of the cells was measured by rhodamine-123 (Fig. 5G and 5H). A decrease in the mean fluorescence intensity was observed after treating with TNF- α , which was abolished by CPS-A pre-treatment. The data indicated that CPS-A relieved TNF- α -induced L02 cells apoptosis, which was accompanied by the changes in mitochondrial membrane potential.

3.11. CPS-A regulated the expression of TNF- α receptors

The biological activities of TNF- α , mainly mediated by TNFR1, plays a crucial role in a range of biological processes such as cell injury, antagonism of viral activity and fibroblast proliferation (Peltzer, Darding, & Walczak, 2016). TNFR2 mainly transmits the proliferation signals of thymus cells and NK lymphocytes (Chen et al., 2013). Compared with the control group, the gene expression of TNFR1 in the model group was significantly elevated. CPS-A (100 μ g/mL) led to a significant decrease in TNF- α -induced L02 injury in mRNA expression (Fig. 6A). Meanwhile, the evident

change of TNFR2 hardly emerged in mRNA expression. Furthermore, TNFR1 expression was significantly raised after stimulation with TNF- α , compared with the control group. After treatment with 10 mM of GSH, TNFR1 expression was significantly lower than that of the model group. Moreover, CPS-A pre-treatment decreased the expression of TNFR1 in a dose-dependent manner. Lastly, there was no significant change in TNFR2 expression (Fig. 6B and 6C).

3.12. CPS-A inhibited TNFR1 promoter activity

In this study, the fluorescence intensity of luciferase reporter genes reflected the activity of promoter by inserting DNA sequence of gene promoter of TNFR1 into pGL3 luciferase reporter vector. The pGL3-TNFR1 promoter vectors were constructed by inserting the promoter regions ~1.8 kb upstream of transcription start site in TNFR1 genes into pGL3-Basic vector between MluI and XhoI sites, and then were transferred into L02 cells (Fig. 6D). Meanwhile, pGL3-Basic and pGL3-SV40 were transferred into L02 cells as the negative and positive controls. Fig. 6E indicated that the transfection was successful because the luciferase intensity in the positive control group was 15.8 times higher than that of the negative control group. The promoter activity was increased by one-fold by the treatment of TNF- α , compared with the control group. In addition, compared with the model group, CPS-A (25, 50, and 100 $\mu\text{g}/\text{mL}$) significantly lowered the activities of TNFR1 promoter with the inhibition rates of 15.8%, 24.8%, and 44.9%, respectively.

4. Discussion

A purified polysaccharide (CPS-A) was obtained from cultured *C. sinensis* mycelia in the current study. Fractions with large molecular weight were precipitated by 65% ethanol

and then removed. Fractions with relatively low molecular weight were used in the study to avoid strong immunity reaction *in vivo* during the further study. Finally, CPS-A was obtained, and the measurements indicated that CPS-A was composed of $\rightarrow 2$)- β -D-Manp-(1 \rightarrow , $\rightarrow 4$)- α -D-Glcp-(1 \rightarrow residues in the straight chain, and $\rightarrow 2,4$)- β -D-Manp-(1 \rightarrow residues in the side chain with the ratio of 9:2. Different from CPS-1, a glucomannogalactan with the monosaccharide composition of glucose: mannose: galactose=2.8:2.9:1 (Wang et al., 2009), the monosaccharide composition of CPS-A included only glucose and mannose. The fundamental findings in the present study could promote further research on structure-activity relationships of CPS-A, as well as other similar polysaccharides.

TNF- α induces mitochondrial abnormality and excessive ROS production that leads to hepatocyte injury and apoptosis by sequentially activating the TNFR1/ROS/Mfn2 pathway (Li et al., 2014). It has been reported that oxidative stress is an important factor inducing mitochondrial dysfunction, which results in excessive production of ROS and the imbalance of oxidation system and antioxidation system (Simon, Haj-Yehia, & Levi-Schaffer, 2000) The mitochondrial pores oxidized by excessive ROS disrupt the mitochondrial membrane potential, leading to cytochrome c release (Wang et al., 2015; Park et al., 2014). The present study revealed that pre-treatment with CPS-A was able to reverse altered mitochondrial membrane potential to normal levels in a dose-dependent manner. Moreover, we also found that CPS-A reduced TNF- α -induced ROS production. Taken together, this study suggests that CPS-A is able to regulate mitochondrial membrane potential and ROS production to relieve oxidative stress.

Bcl-2 family play a central role in apoptosis, and are apoptotic regulatory proteins that control the mitochondrial cell death pathway (Wang et al., 2014a). Bcl-2 family members locate on the mitochondrial membrane, which could alter the permeability of the mitochondrial membrane. Among Bcl-2 family members, Bcl-2 is an anti-apoptotic protein,

while Bax and Bid are pro-apoptotic proteins. The balance between Bcl-2 and Bax is critical for the induction of apoptosis to determine whether to undergo apoptosis (Wang & Xia, 2016; Quast, Berger, & Eberle, 2013). Apoptosis is dependent on the expression of Bax, and abrogated by the overexpression of Bcl-2. In particular, Bax/Bcl-2 regulates the release of cytochrome c that activates caspase-9 and the downstream effector caspase-3, eventually inducing apoptosis (Song et al., 2015; Nicholson & Thornberry, 2003). In the present study, we demonstrated that pre-treatment with CPS-A significantly attenuated TNF- α -induced Bax and Bid expression, and increased Bcl-2 expression; additionally, CPS-A had a synergistic effect with the reduction of caspase-3 and caspase-9. These findings suggest that CPS-A is most likely to suppress TNF- α -induced apoptosis through the activation of Bcl-2 and the inhibition of Bax generation.

Mitochondrial permeability transition is a vital step in the induction of cellular apoptosis (Upur et al., 2011). Mfn2 encodes an integral outer mitochondrial network that regulates mitochondrial metabolism, oxidative stress, and cell death *etc* (De Brito & Scorrano, 2008). Loss or down-regulation of Mfn2 has been found in energy dysmetabolism-related diseases. In this study, CPS-A showed reversing effects against TNF- α -induced decreases in both mRNA and protein expression of Mfn2, which indicated that CPS-A might reverse energy dysmetabolism-related mitochondrial damage. PGC-1 α has been well-documented to regulate Mfn2 activation in hepatocytes, which is based on the observation that TNF- α inhibited both expression of Mfn2 and PGC-1 α (Li et al., 2014).

TNF- α regulates cell survival and apoptosis, depending on the cell type and biological context (Hehlgans & Pfeffer, 2005). TNF- α production has been shown to be increased in TNF- α -induced hepatocyte injury and apoptosis both *in vitro* and *in vivo* during ischemia reperfusion, which suggests that TNF- α promotes hepatocyte apoptosis under ischemia reperfusion conditions (Li et al., 2014). TNF- α activity is mediated by two distinct cell

surface receptors: TNFR1 and TNFR2. TNFR1 presents in normal hepatocytes, and is up-regulated upon apoptosis in response to liver injury, while TNFR2 is rarely expressed in normal liver cells (Desmouliere & Guyot, 2004). We demonstrated that CPS-A treatment reduced the overexpression of TNF- α receptor induced by TNF- α via the type-1 receptor, but not the type-2 receptor. Therefore, these findings suggest that CPS-A has protective effects on liver parenchyma cells against liver damage to maintain the normal function in liver.

In summary, our study demonstrates that CPS-A exhibits protective effects against TNF- α -induced mitochondria abnormality via TNFR1/ROS/Mfn2 pathway; CPS-A is able to efficiently mediate the expression of key factors, such as Mfn2, PGC-1 α , and TNFR1, to attenuate the generation of ROS and mitochondria-related apoptosis cytokines. The present study provides new insight into the mechanisms underlying the function of CPS-A against TNF- α induced mitochondria abnormality and L02 cells apoptosis. Combined with our earlier study (Wang et al., 2014b; Wang et al., 2015), *Cordyceps sinensis* mycelia polysaccharide is approved for Phase II clinical trials now. The dosage is 0.25 g \times 5 pills, three times a day, oral drug administration. We believed that in addition to reducing renal injury, CPS-A may have additional therapeutic benefits against liver diseases that are associated with mitochondria abnormality, oxidation, and apoptosis.

Conflict of Interest

The authors confirm that there are no conflicts of interest.

Acknowledgments

This work was supported by the 2011 National Natural Science Foundation (No. 81173527), and 2012 Youth Fund of National Natural Science Foundation (No. 81202900). This work was also supported by the Industry-University-Institute Cooperation Project of Science & Technology Department of Jiangsu provincial government (No.BY2015072-01) and the Fundamental Research Funds for the Central Universities (No.2016ZPY002). A

project funded by the Priority Academic Program Development of Jiangsu Higher Education Institutions (PAPD).

References

- Antonio, Z., Isabel, H. M., David, S., & Pablo, M. J. (2015). Mitofusin 2 as a driver that controls energy metabolism and insulin signaling. *Antioxidants & Redox Signaling*, 22(12), 1020-1031.
- Bach, D., Pich, S., Soriano, F. X., Vega, N., Baumgartner, B., Oriola, J., et al. (2003). Mitofusin-2 determines mitochondrial network architecture and mitochondrial metabolism. *Journal of Biological Chemistry*, 278, 17190-17197.
- Busquets, S., Aranda, X., Ribas-Carbo, M., Azcon-Bieto, J., Lopez-Soriano, F. J., & Argiles, J. M. (2003). Tumor necrosis factor-alpha uncouples respiration in isolated rat mitochondria. *Cytokine*, 22, 1-4.
- Cai, W., Xie, L., Chen, Y., & Zhang, H. (2013). Purification, characterization and anticoagulant activity of the polysaccharides from green tea. *Carbohydrate Polymers*, 92(2), 1086-1090.
- Chen, J., Yao, D., Yuan, H., Zhang, S., Tian, J., Guo, W., et al. (2013). *Dipsacus asperoides* polysaccharide induces apoptosis in osteosarcoma cells by modulating the PI3K/Akt pathway. *Carbohydrate Polymers*, 95, 780-784.
- Chen, X., Wu, X., Zhou, Q., Howard, O. M. Z., Netea, M. J., & Oppenheim, J. J. (2013). TNFR2 is critical for the stabilization of the CD4(+)Foxp3(+) regulatory T cell phenotype in the inflammatory environment. *Journal of Immunology*, 190(3), 1076-1084.
- Chen, Y. B., Lv, L., Jiang, Z., Yang, H., Li, S., & Jiang, Y. (2013). Mitofusin 2 Protects Hepatocyte Mitochondrial Function from Damage Induced by GCDCA. *PloS one*, 8(2), 108-115.
- Ciucanu, I., & Kerek, F., (1984). A simple and rapid method for the permethylation of

- carbohydrates. *Carbohydrate research*, 131(2), 209-217.
- Dang, Z., Feng, D., Liu, X., Yang, T., Guo, L., Liang, J., et al. (2013). Structure and antioxidant activity study of sulfated acetamido-polysaccharide from *Radix hedysari*. *Fitoterapia*, 89, 20–32
- Dai, J., Wu, Y., Chen, S. W., Zhu, S., Yin, H. P., Wang, M., et al. (2010). Sugar compositional determination of polysaccharides from *Dunaliella salina* by modified RP-HPLC method of precolumn derivatization with 1-phenyl-3-methyl-5-pyrazolone. *Carbohydrate Polymers*, 82, 629–35.
- De Brito, O. M., & Scorrano, L. (2008). Mitofusin 2 tethers endoplasmic reticulum to mitochondria. *Nature*, 456(7222), 605-610.
- Desmouliere, A., & Guyot, C. C. (2004). The stroma reaction myofibroblast: a key player in the control of tumor cell behavior. *International Journal of Developmental Biology*, 48(5-6), 509-517.
- Hansen, M. B., Nielsen, S. E., & Berg, K. (1989). Re-examination and further development of a precise and rapid dye method for measuring cell growth/cell kill. *Journal of Immunological Methods*, 119, 203–210.
- Hehlhans, T., & Pfeffer, K. (2005). The intriguing biology of the tumor necrosis factor/tumor necrosis factor receptor superfamily: players, rules and the games. *Immunology*, 115, 1–20.
- Hikita, H., Kodama, T., Tanaka, S., Saito, Y., Nozaki, Y., Nakabori, T., et al. (2015). Activation of the mitochondrial apoptotic pathway produces reactive oxygen species and oxidative damage in hepatocytes that contribute to liver tumorigenesis. *Cancer Prevention Research*, 8(8), 693-701.
- Hu, H., Liang, H., & Wu, Y. (2015). Isolation: purification and structural characterization of polysaccharide from *Acanthopanax brachypus*. *Carbohydrate Polymers*, 127, 94–100.
- Kathirvel, E., Morgan, K., French, S. W., & Morgan, T. R. (2013). Acetyl-L-carnitine and

- lipoic acid improve mitochondrial abnormalities and serum levels of liver enzymes in a mouse model of nonalcoholic fatty liver disease. *Nutrition Research*, 33(11), 932-941.
- Lemasters, J. J., & Nieminen, A. L. (1997). Mitochondrial oxygen radical formation during reductive and oxidative stress to intact hepatocytes. *Bioscience Reports*, 17, 281-291.
- Li, B., Dobruchowska, J. M., Gerwig, G. J., Dijkhuizen, L., & Kamerling, J. P. (2013). Structural investigation of water-soluble polysaccharides extracted from the fruit bodies of *Coprinus comatus*. *Carbohydrate Polymers*, 91(1), 314–321.
- Li, J., Ke, W., Zhou, Q. Wu, Y. Z., Luo, H., Zhou, H., et al. (2014). Tumor necrosis factor- α promotes liver ischemia-reperfusion injury through the PGC-1 α /Mfn2 pathway. *Journal of Cellular and Molecular Medicine*, 18(9), 1863-1873.
- Liu, W., Liu, Y. M., Zhu, R., Yu, J. P., Lu, W. S., Pan, C., et al. (2016). Structure characterization, chemical and enzymatic degradation, and chain conformation of an acidic polysaccharide from *Lycium barbarum* L. *Carbohydrate Polymers*, 147, 114–124.
- Makarova, E. N., Patova, O. A., Shakhmatov, E. G., Kuznetsov, S. P., & Ovodov, Y. S. (2013). Structural studies of the pectic polysaccharide from Siberian fir (*Abies sibirica* Ledeb.). *Carbohydrate Polymers*, 92, 1817–1826.
- Nicholson, D. W., & Thornberry, N. A. (2003). Life and death decisions. *Science*, 299, 214–15.
- Nie, S., Cui, S., Phillips, A., Xie, M., Phillips, G., Al-Assaf, S., et al. (2011). Elucidation of the structure of a bioactive hydrophilic polysaccharide from *Cordyceps sinensis* by methylation analysis and NMR spectroscopy. *Carbohydrate Polymers*, 84(3), 894–899.
- Park, J., Ko, Y. S., Yoon, J., Kim, M. A., Park, J. W., Kim, W. H., et al. (2014). The forkhead transcription factor FOXO1 mediates cisplatin resistance in gastric cancer cells by activating phosphoinositide 3-kinase/Akt pathway. *Gastric Cancer*, 17, 423–30.
- Peltzer, N., Darding, M., & Walczak, H. (2016). Holding RIPK1 on the ubiquitin leash in

- TNFR1 signaling. *Trends in Cell Biology*, 26(6), 445-461.
- Peng, J. H., Li, X. M., Feng, Q., Chen, L., Xu, L. L., & Hu, Y. Y. (2013). Anti-fibrotic effect of *Cordyceps sinensis* polysaccharide: Inhibiting HSC activation, TGF- β 1/Smad signaling, MMPs and TIMPs. *Experimental Biology and Medicine*, 238(6), 668-677.
- Quast, S. A., Berger, A., & Eberle, J. (2013). ROS-dependent phosphorylation of Bax by wortmannin sensitizes melanoma cells for TRAIL-induced apoptosis. *Cell Death and Disease*, 4, 839.
- Ruthes, A. C., Carbonero, E. R., Córdovac, M. M., Baggio, C. H., Santos, A. R. S., Sasaki, G. L., et al. (2013). *Lactarius rufus* (1 \rightarrow 3), (1 \rightarrow 6)- β -d-glucans: Structure, antinociceptive and anti-inflammatory effects. *Carbohydrate Polymers*, 94, 129–136.
- Santos, M. H. H., Higuchi M, d. L., Tucci P, J. F., Garavelo, S. M., Reis, M. M., Antonio, E. L., et al. (2016). Previous exercise training increases levels of PPAR-alpha in long-term post-myocardial infarction in rats, which is correlated with better inflammatory response. *Clinics*, 71(3), 163-168.
- Savag, M. G., Lackman, D. B., & Smolens, J. (1938). The isolation of the components of streptococcal nucleoproteins in serologically active form. *Journal of Biological Chemistry*, 124, 425–436
- Shang, M., Zhang, X., Dong, Q., Yao, J., Liu, Q., & Ding, K. (2012). Isolation and structural characterization of the water-extractable polysaccharides from *Cassia obtusifoliaseeds*. *Carbohydrate Polymers*, 90(2), 827–832.
- Shashidhar, M. G., Giridhar, P., Sankar, K. U., & Manohar, B. (2013). Bioactive principles from *Cordyceps sinensis*: A potent food supplement - A review. *Journal of Functional Foods*, 5(3), 1013-1030.
- Simon, H. U., Haj-Yehia, A., & Levi-Schaffer, F. (2000). Role of reactive oxygen species (ROS) in apoptosis induction. *Apoptosis*, 5, 415–418.

- Song, G. H., Huang, F. B., Gao, J. P., Liu, M. L., Pang, W. B., Li, W. B., et al. (2015). Effects of fluoride on DNA damage and caspase-mediated apoptosis in the liver of rats. *Biological Trace Element Research*, *166*(2), 173-182.
- Sourav, K. M., Soumya, C., & Samiran, S. G. (2014). Isolation and characterization of extracellular polysaccharide Thelebolan produced by a newly isolated psychrophilic antarctic fungus *Thelebolus*. *Carbohydrate Polymers*, *104*, 204-212.
- Upur, H., Yusup, A., Baudrimont, I., Umar, A., Berke, B., Yimit, D., et al. (2011). Inhibition of cell growth and cellular protein, DNA, and RNA synthesis in human hepatoma (HepG2) cells by ethanol extract of abnormal *Savda Munziq* of traditional Uighur medicine. *Evidence-Based Complementary and Alternative medicine*, *25*, 14-24.
- Wang, B. S., Lee, C. P., Chen, Z. T., Yu, H.M., & Duh, P. D. (2012). Comparison of the hepatoprotective activity between cultured *Cordyceps militaris*, and natural *Cordyceps sinensis*. *Functional Foods*, *4*(2):489-495.
- Wang, T. E., Wang, Y. K., Jin, J., Xu, B. L., & Chen, X. G. (2014a). A novel derivative of quinazoline, WYK431 induces G2/M phase arrest and apoptosis in human gastric cancer BGC823 cells through the PI3K/Akt pathway. *International Journal of Oncology*, *45*,771–781.
- Wang, X., & Xia, M. (2016). 5-Hydroxy-3, 6, 7, 8, 3', 4'-hexamethoxyflavone, a polymethoxyflavone, exerts antitumor effect on PI3K/Akt signaling pathway in human gastric cancer cell BGC-7901. *Journal of Receptors and Signal Transduction*, *36*(5), 471-477.
- Wang, Y., Liu, D., Zhao, H., Jiang, H. X., Luo, C., Wang, M., et al. (2014b). *Cordyceps sinensis* polysaccharide CPS-2 protects human mesangial cells from PDGF-BB-induced proliferation through the PDGF/ERK and TGF-beta1/Smad pathways. *Molecular and Cellular Endocrinology*, *382*(2), 979-988.

- Wang, Y., Wang, Y., Liu, D., Wang, W., Zhao, H., Wang, M., et al. (2015). *Cordyceps sinensis* polysaccharide inhibits PDGF-BB-induced inflammation and ROS production in human mesangial cells. *Carbohydrate Polymers*, 125, 135-145.
- Wang, Y., Wang, M., Ling, Y., Fan, W. Q., Wang, Y. F., & Yin, H. P. (2009). Structural determination and antioxidant activity of a polysaccharide from the fruiting bodies of cultured *Cordyceps sinensis*. *The American Journal of Chinese Medicine*, 37(5), 977-989.
- Wu, Z. D., Puigserver, P., Andersson, U., Zhang, C. Y., Adelmant, G., Mootha, V., et al. (1999). Mechanisms controlling mitochondrial biogenesis and respiration through the thermogenic coactivator PGC-1. *Cell*, 98, 115–124.
- Yan, J. K., Wang, W. Q., & Wu, J. Y. (2014). Recent advances in *Cordyceps sinensis* polysaccharides: mycelial fermentation, isolation, structure, and bioactivities: A review. *Journal of Functional Foods*, 6, 33-47.

Figure captions

Fig. 1 Elution profile of CPS-A in HPGPC with 0.1 M NaNO₃ at a flow rate of 1mL/min on Shodex SB805 and 802 columns. (A) CPS-A is identified as a single symmetrical sharp peak, indicating it is a homogeneous polysaccharide. (B) The standard curve was plotted with GPC software and *M_w* of CPS-A was labeled. (C) *M_n*, *M_w*, *M_z* of CPS-A.

Fig. 2 NMR spectra of CPS-A. (A) ¹H NMR spectrum. (B) ¹³C NMR spectrum. (C) ¹H-¹H COSY spectrum. (D) HSQC spectrum. (E) HMBC spectrum in D₂O.

Fig. 3 Cell Viability Assay. (A) Effects of TNF- α on L02 proliferation assessed by MTT assay. TNF- α was added to L02 cells for incubation of 24 h or 48 h. (B) Effects of GSH on L02 proliferation assessed by MTT assay for 48 h. (C) Effects of CPS-A on L02 proliferation assessed by MTT assay for incubation of 24 h or 48 h. (D) Effects of CPS-A on TNF- α treated L02 proliferation assessed by MTT. Data were expressed as means \pm S.E.M., n = 3. ** $p < 0.01$ vs control. # $p < 0.05$, ## $p < 0.01$ vs model.

Fig. 4 Effects of CPS-A on TNF- α -induced apoptosis in L02 cells. (A) The protein expression of Bid, Bax, and Bcl-2 in TNF- α -induced L02 cells. Columns of the protein expression levels of Bid (B), Bax (C), and Bcl-2 (D) in L02 cells, standardized by β -actin. (E) TNF- α mediated up-regulation of cleaved caspase-3 and cleaved caspase-9 in L02. (F) Columns of the protein expression levels of cleaved caspase-3 and cleaved caspase-9 in TNF- α -induced L02. (G) Nucleolus morphologic changes observed by fluorescent microscope (400 \times). Data were expressed as means \pm S.E.M., n = 3. ** $p < 0.01$ vs control. # $p < 0.05$, ## $p < 0.01$ vs model.

Fig. 5 CPS-A mediated protective effects of mitochondrial associated targets in TNF- α stimulated L02 cells. Cells were treated with 100 ng/mL of TNF- α for 24 h after 12 h pre-incubation with 10 mM of GSH or CPS-A (25, 50, and 100 μ g/mL). (A) Effects of CPS-A on TNF- α induced ROS generation by DCFH-DA. Fluorescence intensity was measured by Accuri C6. (B) Fluorescence values for all groups are normalized to that of untreated cells. (C)

The protein expression levels of Mfn2 in L02 were standardized by β -actin. (D) Columns of the protein expression levels of Mfn2 in TNF- α -induced L02 cells. Real-Time PCR was performed to measure mRNA expression of Mfn2 (E) and PGC-1 α (F), GAPDH was used as the loading control. (G, H) Effects of CPS-A on mitochondrial transmembrane potential in L02 cells. Data represented as means \pm S.E.M., obtained from three independent experiments. ** $p < 0.01$ vs control. # $p < 0.05$, ## $p < 0.01$ vs model.

Fig. 6 CPS-A mediated down-regulation of TNFR1 stimulated by TNF- α in L02 cells. (A) Real-Time PCR was performed to measure mRNA expression of TNFR1 and TNFR2 in TNF- α -induced L02 cells. (B) The protein expression of TNFR1 and TNFR2. (C) Columns of the protein expression levels of TNFRs, standardized by β -actin. (D) Diagram of pGL3-TNFR1 promoter constructs used to express luciferase reporter gene. (E) L02 cells were transfected with pGL3-Basic, pGL3-SV40, and pGL3-TNFR1 promoter constructs and pretreated with CPS-A (25, 50, and 100 $\mu\text{g}/\text{mL}$) for 12 h before incubation with TNF- α (100 ng/mL) for 24 h. Data were expressed as means \pm S.E.M., $n = 3$. ** $p < 0.01$, * $p < 0.05$ vs control. # $p < 0.05$, ## $p < 0.01$ vs model.

Fig. 1

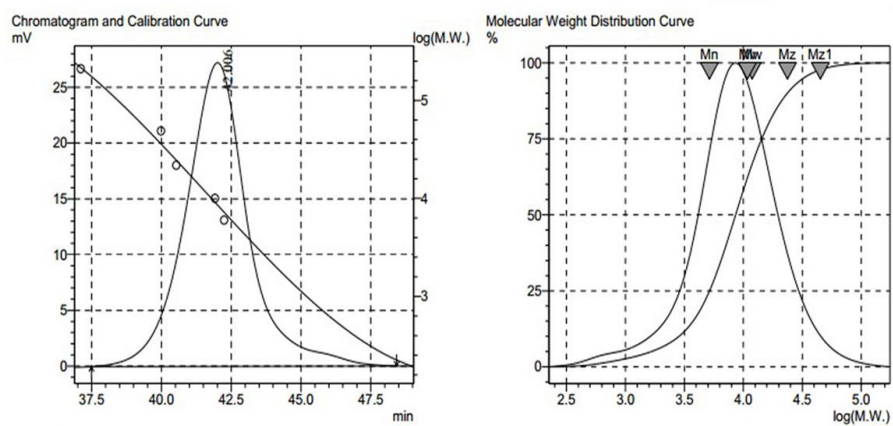
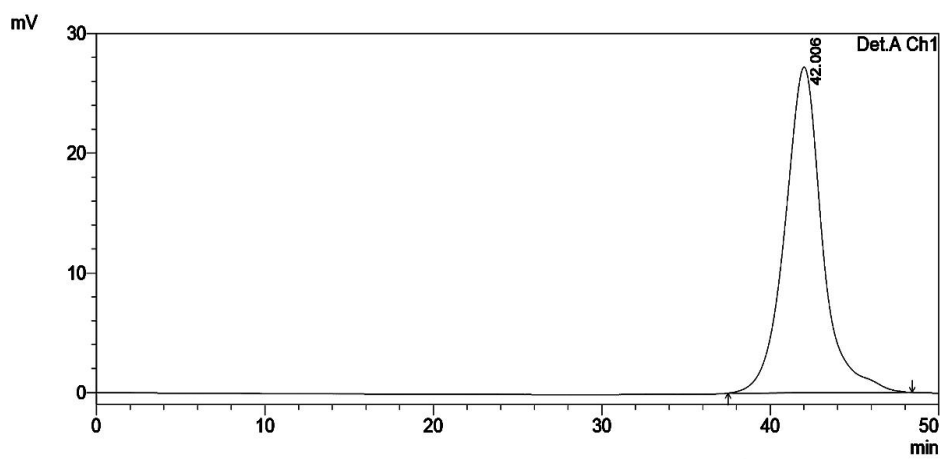
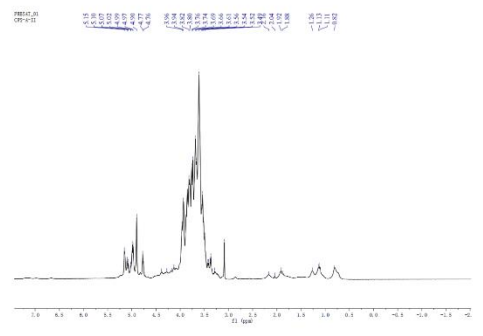
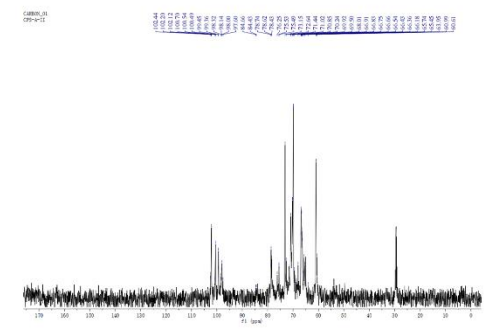


Fig. 2

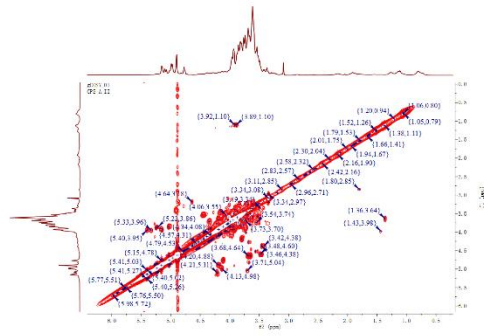
A



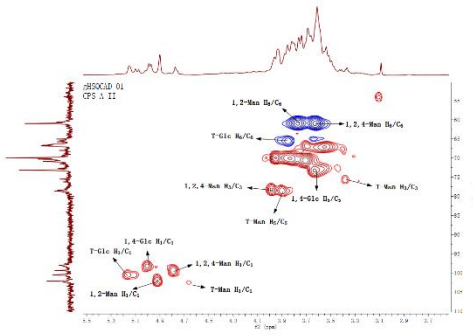
B



C



D



E

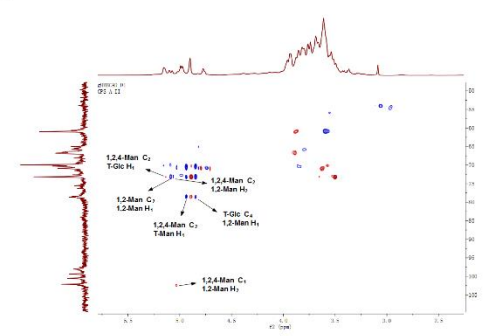


Fig. 3

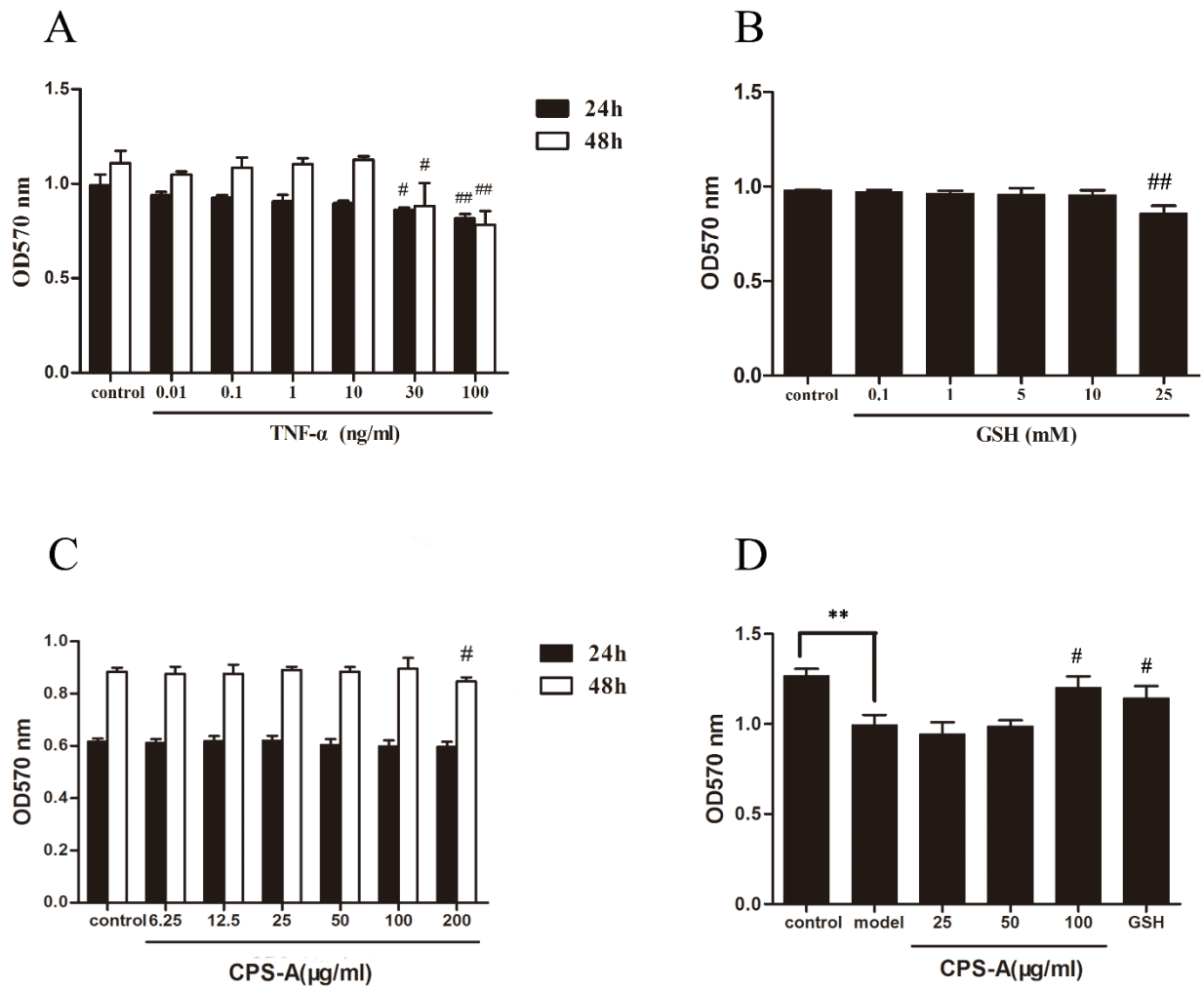
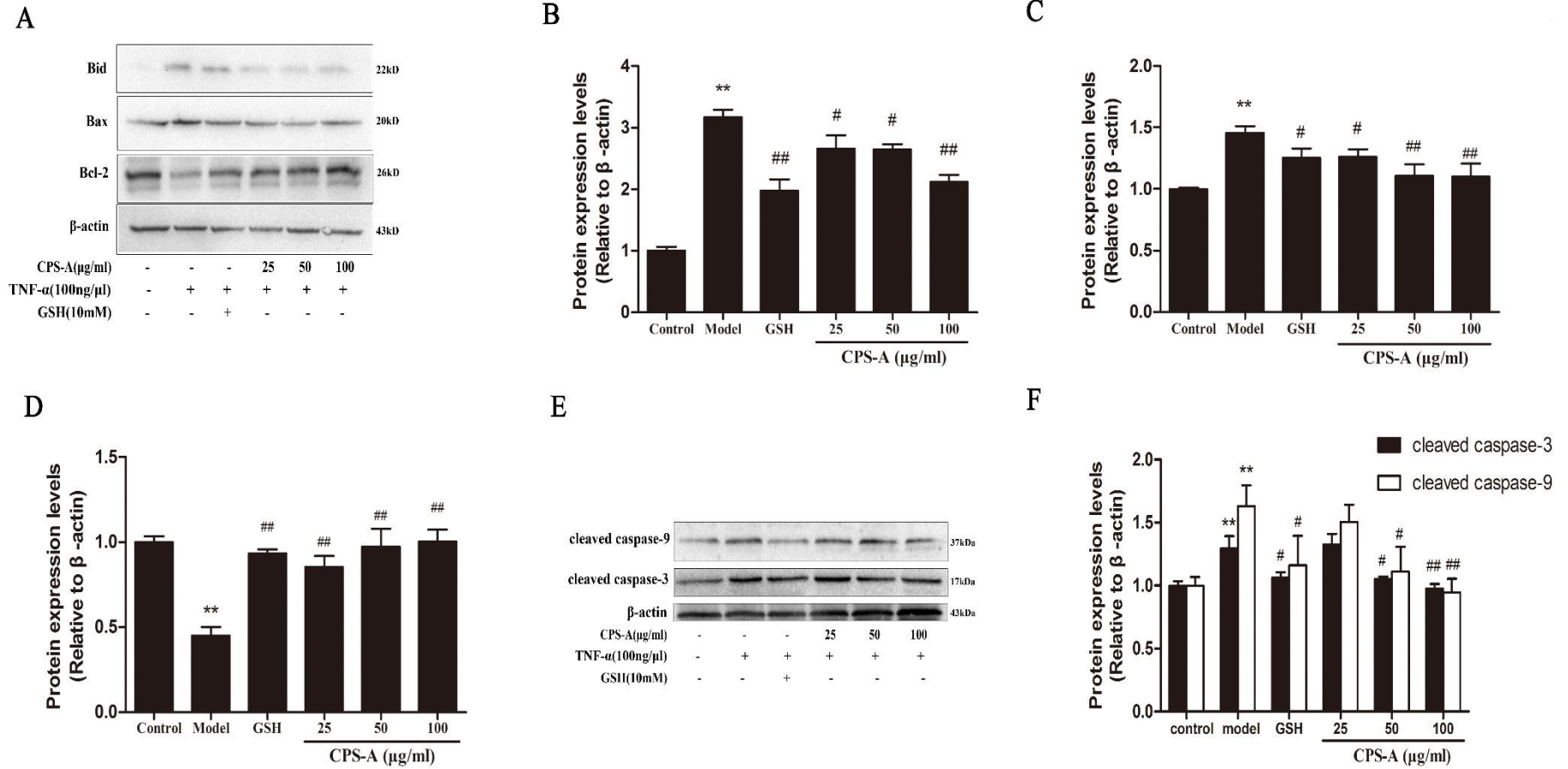


Fig. 4



G

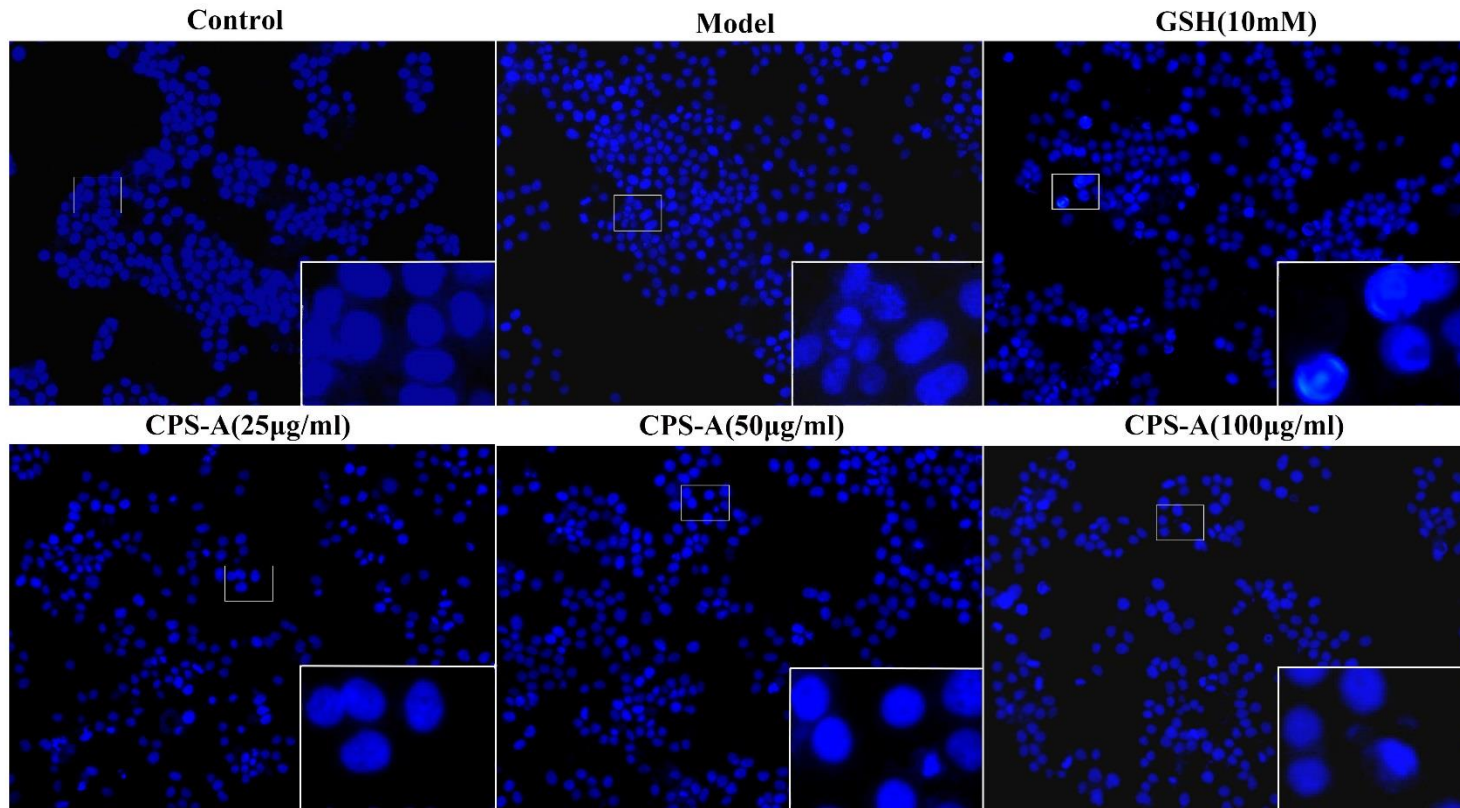


Fig. 5

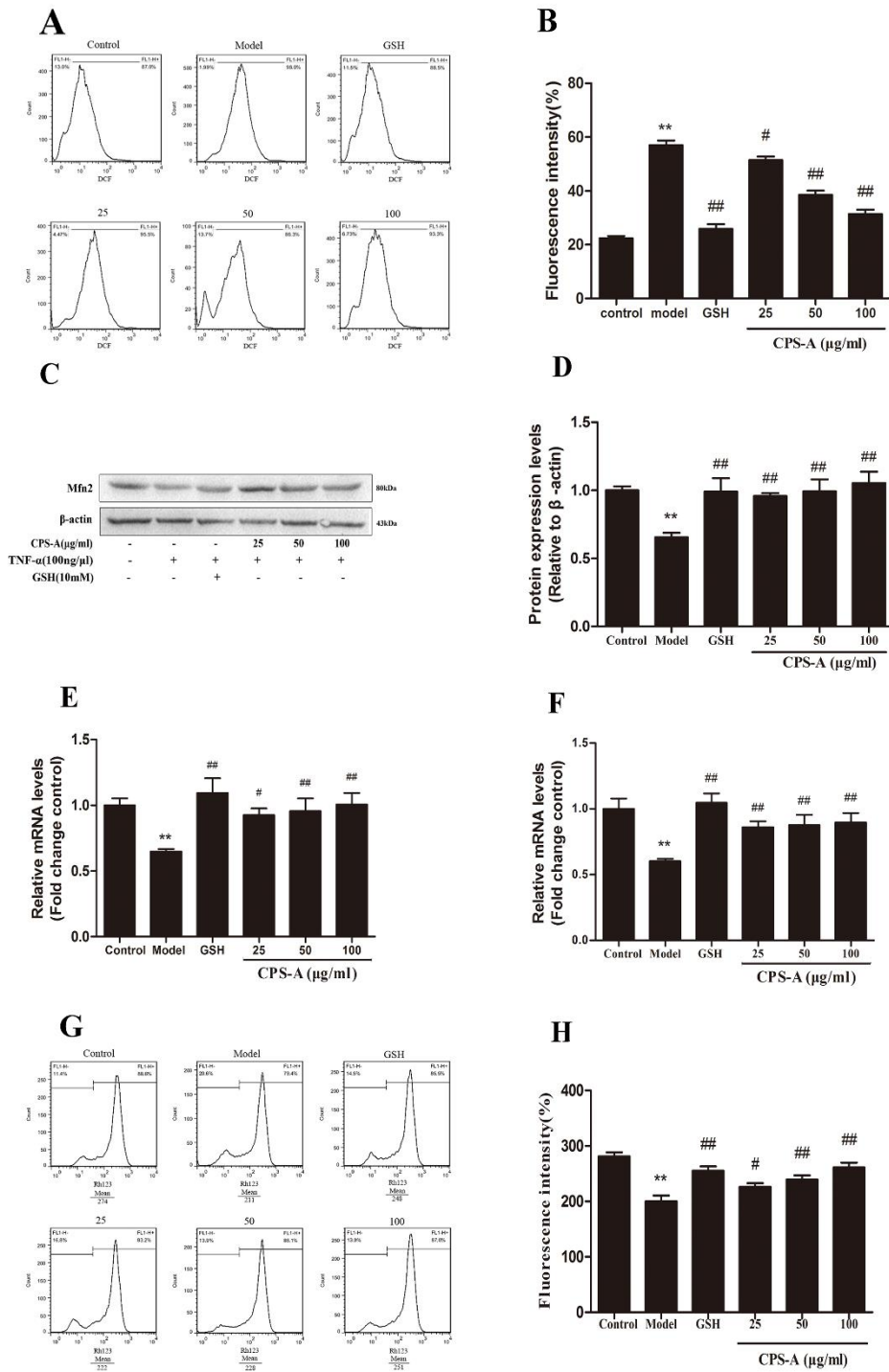


Fig. 6

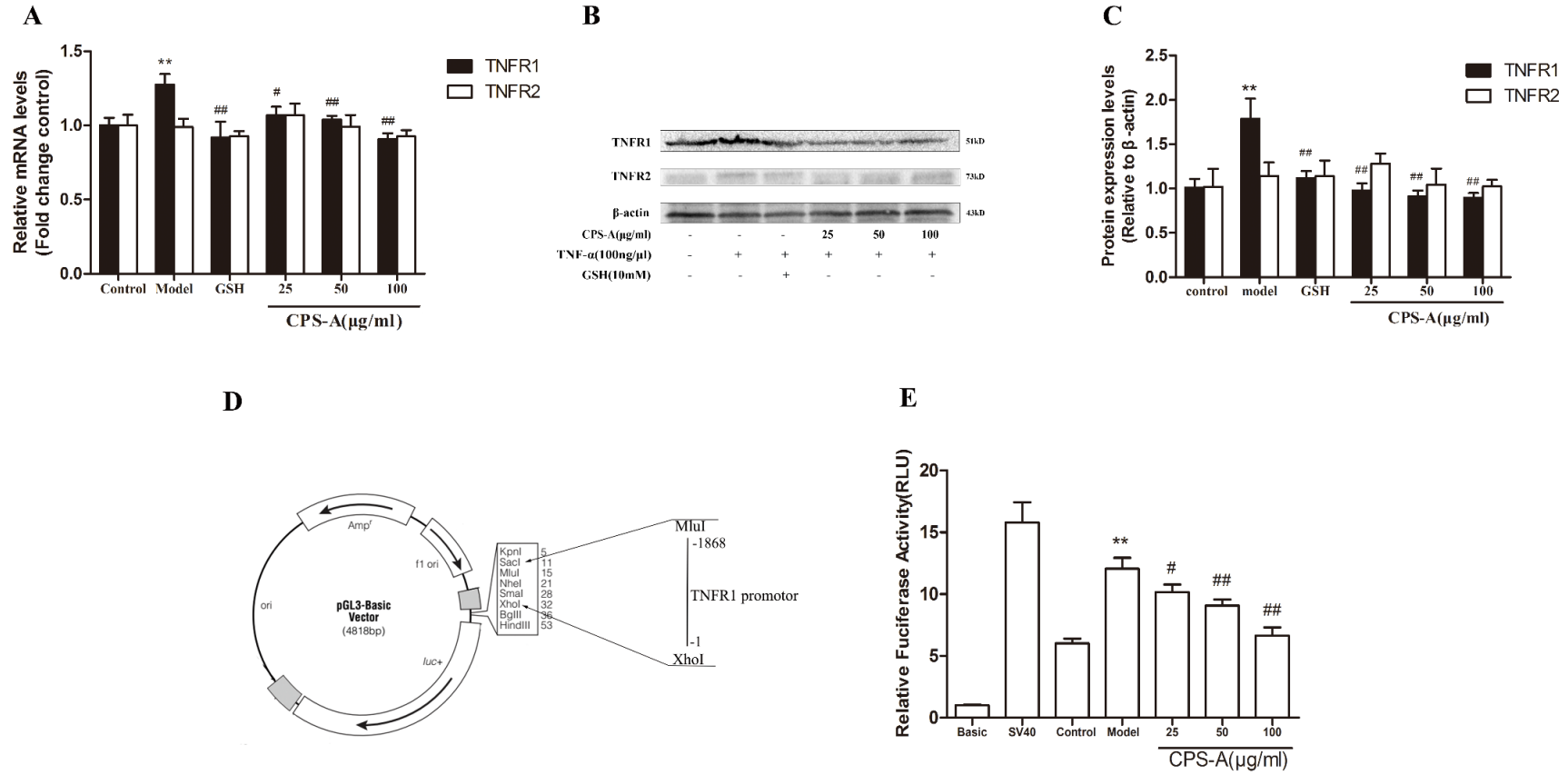


Table 1 GC-MS of main alditol acetate derivatives from the methylated product of CPS-A

Methylated sugars (as alditol acetates)	Type of linkage	Relative molar (%)	Mass fragments (m/z)
2,3,4,6-Me ₄ -Glc _p	Terminal Glc _p	4.4	43,59,71,87,101,117,129,145,161,205
2,3,4,6-Me ₄ -Man _p	Terminal Man _p	17.1	43,59,71,87,101,117,129,145,161,205
3,4,6-Me ₃ -Man _p	1,2-linked Man _p	43.7	43,59,71,87,101,113,129,161,189,205
2,3,6-Me ₃ -Glc _p	1,4-linked Glc _p	27.5	43,57,71,87,101,117,131,142,160,233
3,6-Me ₂ -Man _p	1,2,4-linked Man _p	7.4	43,59,74,87,99,116,129,143,159,189

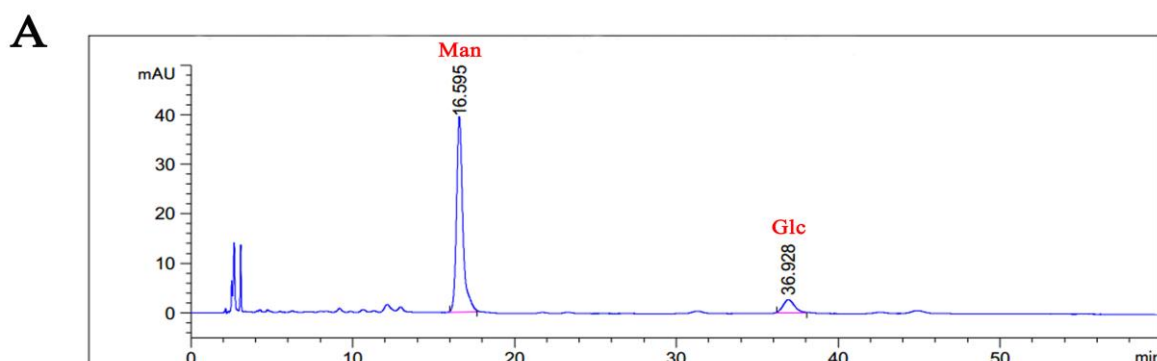
Table 2 ¹³C NMR and ¹H NMR chemical shifts of the main residues from CPS-A in D₂O

Sugar residue	$\delta^{13}\text{C}/\ ^1\text{H}$ (ppm)					
	1	2	3	4	5	6
α -D-Glc-(1→	100.54	70.85	72.64	69.30	71.48	64.74
	5.15	3.56	3.69	3.09	3.74	3.80
β -D-Man-(1→	102.20	69.50	73.15	66.48	78.74	65.01
	4.99	4.76	3.69	3.61	3.90	3.76
→4)- α -D-Glc-(1→	100.49	71.02	75.49	78.76	69.92	60.99
	5.10	3.54	3.85	3.56	3.80	3.82

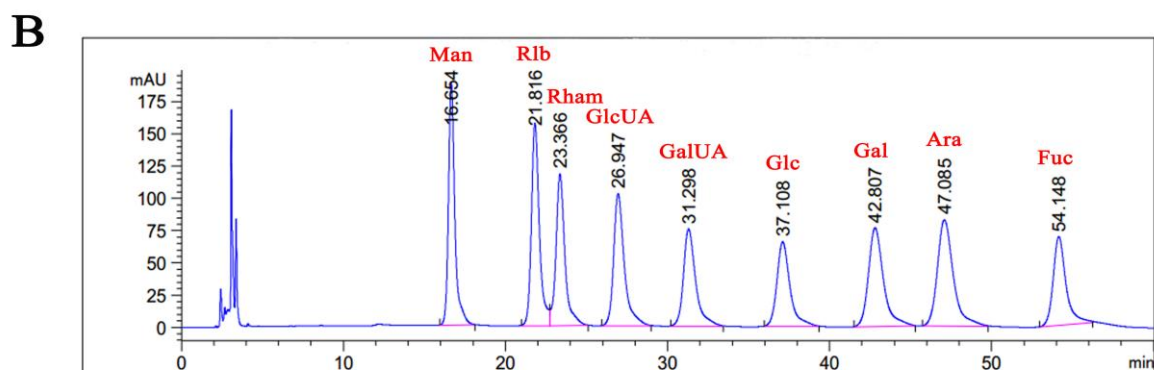
→2)-β-D-Man-(1→	102.12	78.61	70.35	66.83	78.62	60.99
	4.85	5.03	3.66	3.80	3.85	3.61
→2,4)-β-D-Man-(1→	102.20	73.15	78.43	97.60	98.00	60.61
	4.90	84.43	3.66	3.66	3.80	3.66

Supplement data

Data 1 HPLC image of monosaccharide composition of CPS-A.



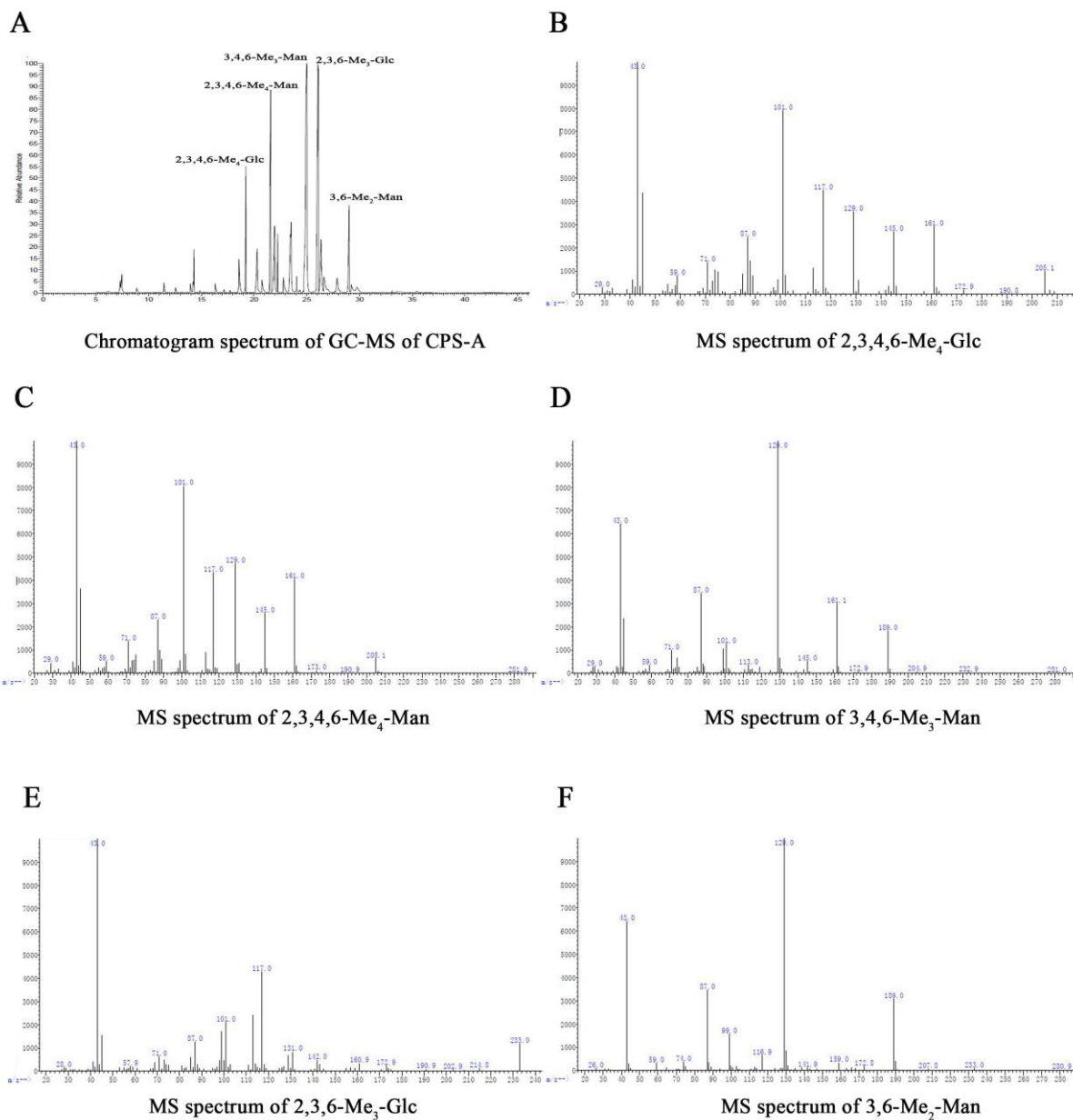
HPLC image of monosaccharide composition of CPS-A



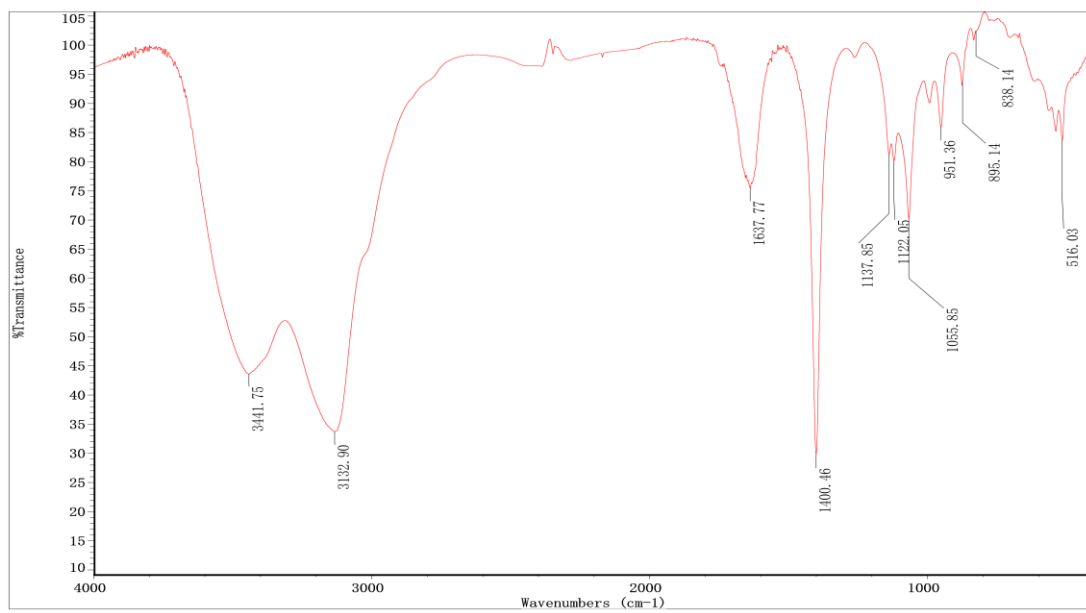
HPLC image of standard monosaccharides

Data 2 Graphs of GC-MS of CPS-A after methylation reaction. (A) The chromatogram spectrum of GC-MS of CPS-A. (B) MS spectrum of 2,3,4,6-Me₄-Glc, the retention time was at 19.23 min. (C) MS spectrum of 2,3,4,6-Me₄-Man, the retention time was at 21.58 min. (D) MS spectrum of 3,4,6-Me₃-Man, the retention

time was at 25.00 min. (E) MS spectrum of 2,3,6-Me₃-Glc, the retention time was at 26.07 min. (F) MS spectrum of 3,6-Me₂-Man, the retention time was at 29.03 min.



Data 3 The FT-IR spectrum of CPS-A.



The FT-IR spectrum of CPS-A